Coupled Systems Mechanics, *Vol. 12, No. 1 (2023) 83-102*
https://doi.org/10.12989/csm.2023.12.1.083

The plate on the nonlinear dynamic foundation under moving load

Phuoc T. Nguyen*[1], Thieu V. Vi[1a], Tuan T. Nguyen[1b] and Van T. Vu[2c]

[1]Faculty of Civil Engineering, Ho Chi Minh City Open University,
97 Vo Van Tan, Ho Chi Minh City 700000, Vietnam
[2]Department of Civil Engineering, Ho Chi Minh City University of Achitecture,
196 Pasteur, Ho Chi Minh City 700000, Vietnam

(Received February 14, 2022, Revised February 28, 2023, Accepted March 3, 2023)

Abstract. First introduced in 2016, the dynamic foundation model is an interesting topic in which the foundation is described close to reality by taking into account the influence of the foundation mass in the calculation of oscillation and is an important parameter that should be considered. In this paper, a follow-up investigation is conducted with the object of the Mindlin plate on a nonlinear dynamic foundation under moving loads. The base model includes nonlinear elastic springs, linear Pasternak parameters, viscous damping, and foundation mass. The problem is formulated by the finite element analysis and solved by the Newmark-β method. The displacement results at the center of the plate are analyzed and discussed with the change of various parameters including the nonlinear stiffness, the foundation mass, and the load velocity. The dynamic response of the plate sufficiently depends on the foundation mass.

Keywords: dynamic analysis; foundation mass; moving load; nonlinear dynamic foundation model; plate on foundation

1. Introduction

The foundation model was first proposed by Winkler in 1867, this is the most basic model and is still widely applied in designs, calculations, and researches up to the present. From the development demands in construction, especially crucial for high-speed transportation systems such as the road-foundation-vehicles system, or airplane-runway system, it can be seen the model plays a very important role to most accurately predict the behavior of the structure. Since then, a series of studies have been born and are expanding, such as the infinite plate on the elastic foundation with variant velocity (Huang and Thambiratnam 2001); the investigation of the dynamic response of the plate and the resonance with parameters of the foundation stiffness, the

*Corresponding author, Associate Professor, E-mail: phuoc.nguyen@ou.edu.vn
[a]Graduate Student, E-mail: thieuvv@yahoo.com
[b]Ph.D. Student, E-mail: tuannt.21ac@ou.edu.vn
[c]Associate Professor, E-mail: van.vutan@uah.edu.vn

http://www.techno-press.org/?journal=csm&subpage=8 ISSN: 2234-2184 (Print), 2234-2192 (Online)

velocity, and frequency of the moving load (Huang *et al.* 2002); the investigation of the viscosity of the foundation and comparison with the elastic system, using Fourier transform for analysis of the infinite plate (Kim and McCullough 2003); the dynamic response of the laminated composite plates with varying parameters of the sprung mass, analyzed by finite element model (Mohebpour and Ahmadzadeh 2011); the study of the effects of velocity (with its varying tangents) and its initial value on the dynamic response of the plate (Li *et al.* 2013); the study of free vibration of elastically restrained Timoshenko beam on an arbitrary variable Winkler foundation and under axial load (Ghannadiasl and Mofid 2015); the analysis of solution for the elastic bending of beams lying on a linearly variable Winkler support (Froio *et al.* 2017); the analysis of FG-CNT reinforced composite conical panel subjected to moving load using Ritz method (Kiani 2017); the study of the dynamics of FG-CNT reinforced composite cylindrical panel subjected to moving load (Kiani 2017); the study of critical velocities of a beam on nonlinear elastic foundation under harmonic moving load (Froio *et al.* 2017); the analytical solution for the elastic bending of beams lying on a linearly variable Winkler support (Froio and Rizzi 2017); the analytical solution for a finite Euler-Bernoulli beam with single discontinuity in section under arbitrary dynamic loads (Yu *et al.* 2018); the analysis of a uniform Bernoulli-Euler beam on Winkler foundation subjected to harmonic moving load (Jiya and Shaba 2018); the study of the dynamics of a beam on a bilinear elastic foundation under harmonic moving load (Froio *et al.* 2018); the dynamic response of a finite beam resting on a Winkler foundation to a load moving on its surface with variable speed (Beskou and Muho 2018); the influence of graphene platelets on the response of composite plates subjected to a moving load (Kiani 2020); the dynamic response of plates resting on a fractional viscoelastic foundation and subjected to a moving load (Praharaj and Datta 2020); the dynamic response of railway track resting on variable foundation using finite element method (Phadke and Jaiswal 2021); the dynamic analysis of railway track on variable foundation under harmonic moving load (Phadke and Jaiswal 2021); a development of an analytical method for calculating beams on a variable elastic Winkler foundation (Yu *et al.* 2021); the study of free and forced vibrations of graphene platelets reinforced composite laminated arches subjected to moving load (Kiani 2022); the analysis of arbitrary thick graphene platelet reinforced composite plates subjected to moving load using a shear and normal deformable plate model (Jafari and Kiani 2022a); a four-variable shear and normal deformable quasi-3D beam model to analyze the free and forced vibrations of FG-GPLRC beams under moving load (Jafari and Kiani 2022b). However, the lack of connection between the springs, and the discontinuity of the foundation displacement between the loaded and the unloaded part are the existing limitations of this type of model (Teodoru and Muşat 2010).

The above limitations from the Winkler model have been also the motivation for a series of studies to be written to improve and bring the model closer to the real foundation. First of all, it was the solution for connecting the separate springs or taking into account the shear deformation in the foundation. These models all gave good results when analyzing the behavior of plate structures on the foundation under different types of moving loads by different methods, such as the analysis of the two-parameter model (Pasternak foundations) by numerical approach (Ferreira *et al.* 2010); the survey of the beam resting on the Vlasov foundation by numerical method (Teodoru and Muşat 2010); the plate on the Pasternak foundation with 3D analysis based on elastic theory (Liu *et al.* 2017); the study of vibration of orthotropic rectangular plates under the action of moving distributed masses and resting on a variable elastic Pasternak foundation with clamped end conditions (Awodola and Adeoye 2021). After that, a series of extensive studies for the nonlinearity with or without damping of the background model was also performed. In fact, the spring reaction shows a third-order dependence on the vertical displacement. The results obtained from the study show that there was a remarkable difference between the models of nonlinear and linear foundation, such as the laminated plate resting on the nonlinear foundation (Chien and Chen 2005); the investigation of the beam resting on the nonlinear by the Galerkin method (Ding *et al.* 2012); the beam resting on the nonlinear Pasternak foundation with six parameters (Yang *et al.* 2013); the beam resting on the nonuniform linear foundations and bilinear foundation (Jorge *et al.* 2015a, b); the nonuniform beam resting on the nonlinear foundation with varying velocities and loads (Abdelghany *et al.* 2015); the analysis of large displacement of the beam resting on the nonlinear foundation (Froio *et al.* 2017); the beam resting on the nonlinear foundation with primary resonance study (Karahan and Pakdemirli 2017); the analysis of the nonlinear dynamics (Zhou *et al.* 2017); the beam resting on linear, bilinear, and nonlinear models by finite element approach with critical and ranges of velocities (Rodrigues *et al.* 2018); the infinite beam resting on the nonlinear foundation with large deflections (Ahmad *et al.* 2018); the dynamic response of plates resting on a fractional viscoelastic foundation and subjected to a moving load (Praharaj and Datta 2020); the effects of initial compression/tension, foundation damping and pasternak medium on the dynamics of shear and normal deformable GPLRC beams under moving load (Wang and Kiani 2022).

Most recently, when considering the effects of the mass of the foundation on the dynamic structures but was ignored, a new model of foundation that considered the theoretical influence of the foundation mass was suggested to analyze the dynamic response of the superstructures resting on the foundation (Nguyen and Pham 2016, Nguyen *et al.* 2016a, b, Nguyen *et al.* 2020a, b) and was tested using a simple model (Pham *et al.* 2018) for the results of the foundation mass in oscillation participation had a remarkable influence on the dynamic properties of the system. This is close to reality because the foundation always has a density and oscillates with the structures subjected to dynamic loads, causing a specific inertia force and acting together with the inertia force of the structure. This influence gradually decreases with the foundation depth because the natural frequency is inversely proportional to the foundation depth in the structural system.

To further study the dynamic foundation model and bring it closer and closer to the real model, this paper presents an investigation on the plate dynamic response resting on nonlinear foundation under moving loads. The applied numerical method is built and developed by the MATLAB programming language to analyze the dynamics of a plate resting on a nonlinear foundation considering the mass. By using the developed numerical method, this paper investigates the influence of different parameters (in other words, they are basic variables can be appeared in reality) on stiffness, mass, shear modulus, viscous damping of the foundation, and the moving load velocity. Moreover, the peak and time-dependent displacements of the center of the plate will be presented and discussed.

2. Methodology and formulation

2.1 The nonlinear dynamic foundation model

A dynamic foundation model including all characteristics of the nonlinear dynamic foundation was suggested by Nguyen *et al.* (2016b) to supplement an important factor, which is the influence of the mass of foundation in oscillation, of the Winkler model types. This idealized model, as shown in Fig. 1, includes the linear elastic stiffness k_l plus nonlinear elastic stiffness k_{nl} (in which the relation of force-displacement is expressed in a cubic term), the parameter of foundation shear

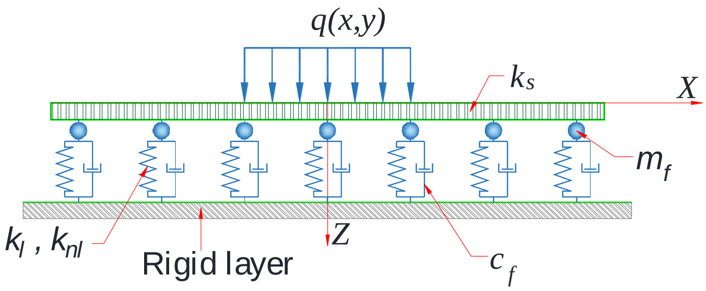

Fig. 1 The dynamic foundation model

layer k_s, the viscous damping c_f and the foundation mass density ρ_f. Based on the principles of dynamic equilibrium, the mass of the foundation is calculated as several lumped masses m_f at the top of the elastic springs which connect the elastic springs with the shear layer. The lumped mass m_f is a parameter that makes the dynamic foundation model significantly different from other models, which are massless ones.

The corresponding force-displacement relation of foundation under pressure $q(x,y,t)$ at the time t, as shown in Fig. 2, can be described and satisfied as the following partial differential equation

$$\frac{\partial N_{x,t}}{\partial x}+\frac{\partial N_{y,t}}{\partial y}+q(x,y,t)-r_0(x,y,t)-m_0(x,y,t)-c_0(x,y,t)=0 \quad (1)$$

In which, total shear force per unit length, which are the connections between the springs and make the loaded and unloaded parts continuously, of a shear layer in x-axis and y-axis, respectively, can be expressed as

$$\begin{aligned} N_{x,t} &= \int_0^1 \tau_{xz,t}\,dz = k_S \frac{\partial w(x,y,t)}{\partial x} \\ N_{y,t} &= \int_0^1 \tau_{yz,t}\,dz = k_S \frac{\partial w(x,y,t)}{\partial y} \end{aligned} \quad (2)$$

The reaction of nonlinear elastic spring, inertia force caused by the foundation mass, and foundation viscous damping resistance, respectively, is given by

$$\begin{aligned} r_0(x,y,t) &= k_l w(x,y,t) + k_{nl} w^3(x,y,t) \\ m_0(x,y,t) &= m_f \frac{\partial^2 w(x,y,t)}{\partial t^2} \end{aligned} \quad (3)$$

We can see that it would be a shortage not to consider the mass of the foundation participating in the oscillation for the dynamic problem (this will be satisfactory in the static problem).

$$c_0(x,y,t) = c_f \frac{\partial w(x,y,t)}{\partial t} \quad (4)$$

The lumped mass $m_f$representing the foundation mass can be written as

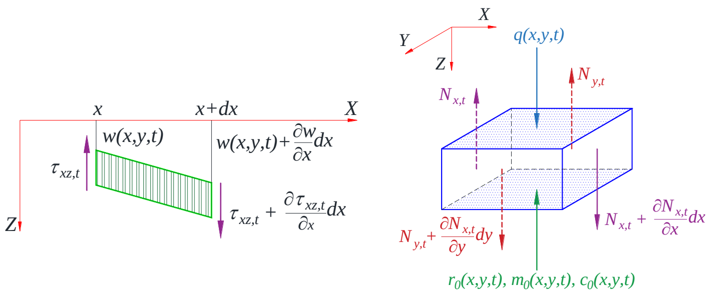

Fig. 2 Dynamic equilibrium on the shear layer: (a) stresses; (b) forces acting

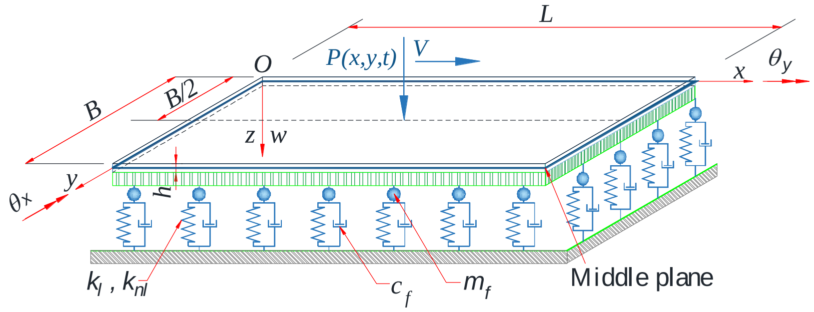

Fig. 3 Model of Mindlin plate on nonlinear dynamic foundation under moving load

$$m_f = \beta \rho_f \tag{5}$$

where $\beta = \alpha_f H_f$ is a dimensionless parameter that depends on the experimental influence factor α_f and the depth of the foundation H_f. This formulation clearly describes how to calculate the mass of the foundation participating in oscillation. In practice, the influence of wheel axle loads will decrease with the depth of the foundation when considering the foundation as a homogeneous elastic half-space. In other words, the mass of the foundation participating in the oscillation decreases with the depth of the foundation.

2.2 Finite element formulation

Consider a Mindlin rectangular plate with width B, length L and uniform thickness h on a nonlinear foundation considering the foundation mass under moving load, as shown in Fig. 3. The quadrilateral four-node element as shown in Fig. 4, $Q4$, is used to develop the numerical method according to the finite element method. Three global degrees of freedom of each node are vertical displacement w, rotation about y -axis and x -axis, θ_x and θ_y, respectively.

Consider the plane in the middle of the plate, the vector of vertical displacement and rotation angles of at any node of the plate can be expressed as

$$\mathbf{d} = \{w \quad \theta_x \quad \theta_y\}^T \tag{6}$$

In order to remove the restriction of the rectangular shape of physical space, the natural

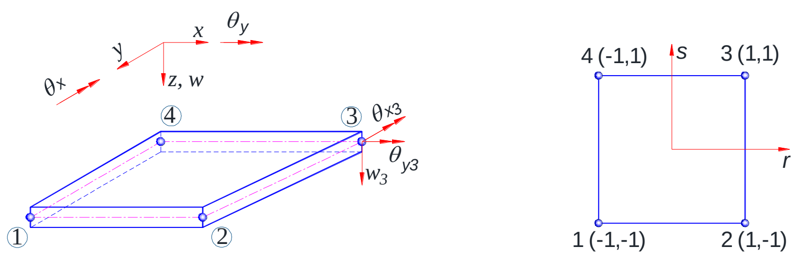

Fig. 4 Quadrilateral four-node elements, $Q4$: (a) in global coordinates; (b) in natural coordinates

coordinates (r, s) are applied for mapping between two coordinate systems for each element. Because the element is isoparametric, the same shape functions are used to interpolate both coordinates and displacements within the considering element. Hence, the shape functions of $Q4$ element, $N_i(i = 1,...,4)$ are defined by Eq. (8), the displacement vector $\boldsymbol{d}$ and the vertical displacement field w in each plate element can be derived from the vector of nodal displacement $\boldsymbol{q}^e$ of the finite elements by using same each specific $N_i(i = 1,...,4)$ shape functions as follows, respectively

$$\begin{aligned} N_i &= \frac{1}{4}(1+rr_i)(1+ss_i) \\ \boldsymbol{d} &= \boldsymbol{N}\boldsymbol{q}^e \\ w &= \boldsymbol{N}_w\boldsymbol{q}^e \end{aligned} \tag{7}$$

in which, $\boldsymbol{N}, \boldsymbol{N}_w$ are the matrices including the shape function as

$$\begin{aligned} \boldsymbol{N} &= \begin{bmatrix} N_1 & 0 & 0 & N_2 & 0 & 0 & N_3 & 0 & 0 & N_4 & 0 & 0 \\ 0 & N_1 & 0 & 0 & N_2 & 0 & 0 & N_3 & 0 & 0 & N_4 & 0 \\ 0 & 0 & N_1 & 0 & 0 & N_2 & 0 & 0 & N_3 & 0 & 0 & N_4 \end{bmatrix} \\ \boldsymbol{N}_w &= \begin{bmatrix} N_1 & 0 & 0 & N_2 & 0 & 0 & N_3 & 0 & 0 & N_4 & 0 & 0 \end{bmatrix} \\ \boldsymbol{q}^e &= \begin{bmatrix} w_1 & \theta_{x1} & \theta_{y1} & w_2 & \theta_{x2} & \theta_{y2} & w_3 & \theta_{x3} & \theta_{y3} & w_4 & \theta_{x4} & \theta_{y4} \end{bmatrix}^T \end{aligned} \tag{8}$$

Under flexural deformation, the elastic strain energy of the element is given by

$$U_p = \frac{1}{2}\int_{V^e} \boldsymbol{\varepsilon}_b{}^T \boldsymbol{\sigma}_b dV^e + \frac{1}{2}\int_{V^e} \boldsymbol{\gamma}^T \boldsymbol{\sigma}_s dV^e = \frac{1}{2}\int_{V^e} \boldsymbol{\varepsilon}_b^T \boldsymbol{D}_b \boldsymbol{\varepsilon}_b dV^e + \frac{1}{2}\kappa_s \int_{V} \boldsymbol{\gamma}^T \boldsymbol{D}_s \boldsymbol{\gamma} dV^e \tag{9}$$

The element flexural and shear strains can be express as

$$\boldsymbol{\varepsilon}_b = z\boldsymbol{B}_b\boldsymbol{q}^e; \quad \boldsymbol{\gamma} = \boldsymbol{B}_s\boldsymbol{q}^e \tag{10}$$

where, $\boldsymbol{B}_b, \boldsymbol{B}_s$ are the strain-displacement gradient matrices to identify curvatures for bending moments and shear forces of the element, respectively, and are obtained by derivation of the shape functions as

$$\begin{aligned} \boldsymbol{B}_b &= \begin{bmatrix} \boldsymbol{B}_{1b} & \boldsymbol{B}_{2b} & \boldsymbol{B}_{3b} & \boldsymbol{B}_{4b} \end{bmatrix} \\ \boldsymbol{B}_s &= \begin{bmatrix} \boldsymbol{B}_{1s} & \boldsymbol{B}_{2s} & \boldsymbol{B}_{3s} & \boldsymbol{B}_{4s} \end{bmatrix} \end{aligned} \tag{11}$$

in which

$$\boldsymbol{B}_{ib}=\begin{bmatrix} 0 & \dfrac{\partial N_i}{\partial x} & 0 \\ 0 & 0 & \dfrac{\partial N_i}{\partial y} \\ 0 & \dfrac{\partial N_i}{\partial y} & \dfrac{\partial N_i}{\partial x} \end{bmatrix};\boldsymbol{B}_{is}=\begin{bmatrix} \dfrac{\partial N_i}{\partial x} & N_i & 0 \\ \dfrac{\partial N_i}{\partial y} & 0 & N_i \end{bmatrix}_{is} \tag{12}$$

Substituting Eq. (10) into Eq. (9), one obtains

$$U_p=\frac{1}{2}\boldsymbol{q}^{eT}\frac{h^3}{12}\int_{A^e}\boldsymbol{B}_b^T\boldsymbol{D}_b\boldsymbol{B}_b dA^e\boldsymbol{q}^e+\frac{1}{2}\boldsymbol{q}^{eT}\kappa_s h\int_{A^e}\boldsymbol{B}_s^T\boldsymbol{D}_s\boldsymbol{B}_s dA^e\boldsymbol{q}^e \tag{13}$$

The element stiffness matrix is obtained by inference from Eq. (13) as

$$\boldsymbol{K}_p^e=\frac{h^3}{12}\int_{A_e}\boldsymbol{B}_b^T\boldsymbol{D}_b\boldsymbol{B}_b dA^e+\kappa_s h\int_{A_e}\boldsymbol{B}_s^T\boldsymbol{D}_s\boldsymbol{B}_s dA^e \tag{14}$$

For states of pure bending and pure twist, the contribution of $\frac{h^3}{12}\int_{A_e}B_b^T D_b B_b dA^e$ is correctly evaluated by all quadrature rules. In order to avoid the trouble of shear locking (in other words, the plate element becomes thin) for Mindlin element caused by positive definite penalty matrix $\kappa_s h\int_{A_e}B_s^T D_s B_s dA^e$, a chosen positive number $\kappa_s = 5/6$ is used for the shear correction factor, D_b , D_s are the flexural and shear rigidity matrices, respectively, given by

$$\boldsymbol{D}_b=\frac{E}{1-\nu^2}\begin{bmatrix} 1 & \nu & 0 \\ \nu & 1 & 0 \\ 0 & 0 & \dfrac{1-\nu}{2} \end{bmatrix};\boldsymbol{D}_s=\frac{E}{2(1+\nu)}\begin{bmatrix} 1 & 0 \\ 0 & 1 \end{bmatrix} \tag{15}$$

In terms of the linear and nonlinear elastic stiffness, the energy caused by elastic strain of the nonlinear foundation is given by

$$U_{nl}=\int_{A^e}\left(\frac{1}{2}k_l w^2+\frac{1}{4}k_{nl}w^4\right)dA^e=\frac{1}{2}\boldsymbol{q}^{eT}\int_{A^e}\boldsymbol{N}_w^T k_l\boldsymbol{N}_w^T dA^e\boldsymbol{q}^e+\frac{1}{4}\boldsymbol{q}^{eT}\int_{A^e}\boldsymbol{N}_w^T k_{nl}\left(\boldsymbol{N}_w\boldsymbol{q}^e\right)^3 dA^e \tag{16}$$

The tangent stiffness matrix of nonlinear foundation for the plate element used in the Newmark-β method and the modified Newton-Raphson method is determined as follows

$$\frac{\partial^2 U_{nl}}{\partial\boldsymbol{q}^e\partial\boldsymbol{q}^e}=\int_{A^e}\boldsymbol{N}_w^T k_l\boldsymbol{N}_w dA^e+3\int_{A^e}\boldsymbol{N}_w^T k_{nl}\left(\boldsymbol{N}_w\boldsymbol{q}^e\right)^2\boldsymbol{N}_w dA^e \tag{17}$$

The elementary linear stiffness matrix and tangent stiffness of foundation can be derived from Eq. (17), respectively, written as

$$\begin{aligned}\boldsymbol{K}_l^e &= \int_{A^e} \boldsymbol{N}_w^T k_l \boldsymbol{N}_w dA^e \\ \boldsymbol{K}_{nl}^e &= 3\int_{A^e} \boldsymbol{N}_w^T k_{nl} \left(\boldsymbol{N}_w \boldsymbol{q}^e\right)^2 \boldsymbol{N}_w dA^e\end{aligned} \tag{18}$$

In connection with the shear layer stiffness, the elastic strain energy of the nonlinear foundation is given by

$$U_s = \frac{1}{2}\int_{A^e} k_s \left[\left(\frac{\partial w}{\partial x}\right)^2 + \left(\frac{\partial w}{\partial y}\right)^2\right] dA^e = \frac{1}{2}\boldsymbol{q}^{eT}\int_{A^e} \boldsymbol{N}_{s,x}^T k_s \boldsymbol{N}_{s,x} dA^e \boldsymbol{q}^e + \frac{1}{2}\boldsymbol{q}^{eT}\int_{A^e} \boldsymbol{N}_{s,y}^T k_s \boldsymbol{N}_{s,y} dA^e \boldsymbol{q}^e \tag{19}$$

By inference from Eq. (19), the stiffness of the shear layer in matrix form is given by

$$\boldsymbol{K}_s^e = \int_{A_e} \boldsymbol{N}_{s,x}^T k_s \boldsymbol{N}_{s,x} dA + \int_{A_e} \boldsymbol{N}_{s,y}^T k_s \boldsymbol{N}_{s,y} dA^e \tag{20}$$

where

$$\begin{aligned}\boldsymbol{N}_{s,x} &= \begin{bmatrix} \frac{\partial N_1}{\partial x} & 0 & 0 & \frac{\partial N_2}{\partial x} & 0 & 0 & \ldots & \frac{\partial N_4}{\partial x} & 0 & 0 \end{bmatrix}; \\ \boldsymbol{N}_{s,y} &= \begin{bmatrix} \frac{\partial N_1}{\partial y} & 0 & 0 & \frac{\partial N_2}{\partial x} & 0 & 0 & \ldots & \frac{\partial N_4}{\partial y} & 0 & 0 \end{bmatrix}\end{aligned} \tag{21}$$

Let ρ be the plate's density, the plate kinetic energy can be manifested as

$$\begin{aligned}T_p &= \frac{1}{2}\int_{V^e} \rho\left(\dot{w}^2 + \left(z\dot{\theta}_x\right)^2 + \left(z\dot{\theta}_y\right)^2\right) dV^e = \frac{1}{2}\int_{A^e} \left(\dot{\boldsymbol{q}}^e\right)^T \left(\boldsymbol{N}^T \boldsymbol{H}\boldsymbol{N}\right)\dot{\boldsymbol{q}}^e dA^e = \\ &= \frac{1}{2}\int_{A^e} \left(\dot{\boldsymbol{q}}^e\right)^T \boldsymbol{M}_p^e \dot{\boldsymbol{q}}^e dA^e\end{aligned} \tag{22}$$

Where M_p^e is the elementary consistent plate's mass matrix and may be written as

$$\begin{aligned}\boldsymbol{M}_p^e &= \int_{A^e} \boldsymbol{N}^T \boldsymbol{H}\boldsymbol{N} dA^e \\ \boldsymbol{H} &= \rho\begin{bmatrix} h & 0 & 0 \\ 0 & \frac{h^3}{12} & 0 \\ 0 & 0 & \frac{h^3}{12} \end{bmatrix}\end{aligned} \tag{23}$$

The kinetic energy of the foundation is given by

$$T_f = \frac{1}{2}\int_{A^e} m_f \dot{w}^2 dA^e = \frac{1}{2}\int_{A^e} \left(\dot{\boldsymbol{q}}^e\right)^T \left(\boldsymbol{N}_w^T m_f \boldsymbol{N}_w\right)\dot{\boldsymbol{q}}^e dA^e = \frac{1}{2}\int_{A^e} \left(\dot{\boldsymbol{q}}^e\right)^T \boldsymbol{M}_f^e \dot{\boldsymbol{q}}^e dA^e \tag{24}$$

in which, M_f^e is the foundation' mass matrix and is given by

$$\boldsymbol{M}_f^e = \int_{A_e} \boldsymbol{N}_w^T m_f \boldsymbol{N}_w dA \tag{25}$$

The dissipation energy of the viscous damping of foundation property can be written as

$$R_f = \frac{1}{2}\int_{A^e} c_f \dot{w}^2 dA^e = \frac{1}{2}\int_{A^e} \left(\dot{\boldsymbol{q}}^e\right)^T \left(\boldsymbol{N}_w^T c_f \boldsymbol{N}_w\right)\dot{\boldsymbol{q}}^e dA^e = \frac{1}{2}\int_{A^e} \left(\dot{\boldsymbol{q}}^e\right)^T \boldsymbol{C}_f^e \dot{\boldsymbol{q}}^e dA^e \tag{26}$$

where C_f^e the damping matrix of the foundation and is given by

$$\boldsymbol{C}_f^e = \int_{A^e} \boldsymbol{N}_w^T c_f \boldsymbol{N}_w dA^e \tag{27}$$

When a concentrated load P travels along the center axis of the plate in x-direction with a constant speed V at each time t, the external load vector can be written as

$$\boldsymbol{p} = \left[P\delta\left(x - Vt\right)\delta\left(y - \frac{B}{2}\right) \quad 0 \quad 0 \right]^T \tag{28}$$

where $\delta(x - Vt)$ and $\delta\left(y - \frac{B}{2}\right)$ are Dirac delta functions that are used to solve a concentrated moving load problem. The potential energy produced in a plate by the moving load may be expressed as

$$V_p = \boldsymbol{p}\boldsymbol{d}^T = \boldsymbol{p}\left(\boldsymbol{N}\boldsymbol{q}^e\right)^T \tag{29}$$

Utilizing the finite element methods, the governing equations can be obtained from the Lagrangian equation as follows

$$\frac{d}{dt}\left(\frac{\partial L}{\partial \dot{q}^e}\right) + \left(\frac{\partial L}{\partial q^e}\right) + \left(\frac{\partial R_f}{\partial \dot{q}^e}\right) = 0 \tag{30}$$

In which, $L = T_p + T_f - \left(U_p + U_{nl} + U_s - V_p\right)$ is the total kinetic and potential energies of the global system. Substituting Eq. (13), (16), (18), (21), (24), (26) and (29) into (30) one obtains

$$\left(\boldsymbol{M}_p^e + \boldsymbol{M}_f^e\right)\ddot{\boldsymbol{q}}^e + \boldsymbol{C}_f^e \dot{\boldsymbol{q}}^e + \left(\boldsymbol{K}_p^e + \boldsymbol{K}_l^e + \boldsymbol{K}_{nl}^e + \boldsymbol{K}_s^e\right)\boldsymbol{q}^e = \boldsymbol{N}^T \boldsymbol{p} \tag{31}$$

Assembling the formulation of all finite elements and identifying the boundary conditions in a discrete system, the motion equation is obtained in the global system

$$\boldsymbol{M}\ddot{\boldsymbol{q}} + \boldsymbol{C}\dot{\boldsymbol{q}} + \boldsymbol{K}\boldsymbol{q} = \boldsymbol{P}\left(t\right) \tag{32}$$

Respectively, the global vector of acceleration, velocity, displacement are represented by $\ddot{q}, \dot{q}, q$; the global matrix of mass, viscous damping and stiffness are represented by M, C, K and the global external load vector is $P(t)$. The Eq. (32) can be solved by employing each time step by integration method based on the Newmark-β algorithm, and integrated by the iteration method of the modified Newton-Raphson.

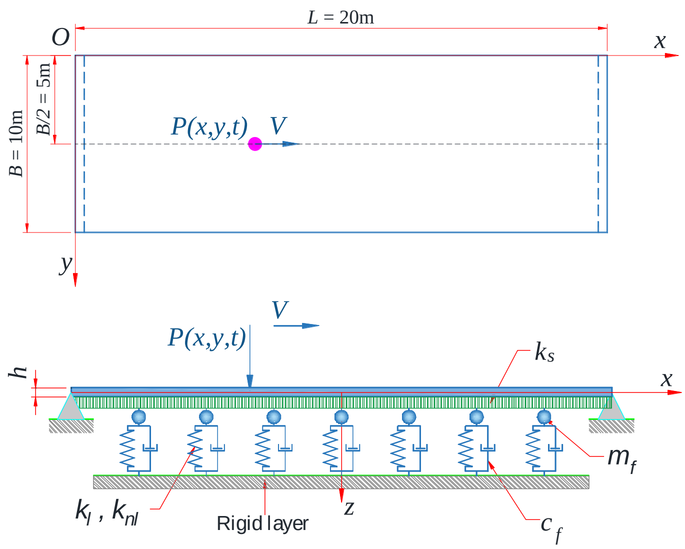

Fig. 5 Model of Mindlin plate on nonlinear dynamic foundation under moving load

3. Numerical results

The purpose of this section is to carry out various numerical examples to study the dynamic properties and the plate responses resting on a nonlinear foundation under moving load considering the mass of the foundation. The first example considers the effects of the nonlinear elastic stiffness of the foundation by different parameters, including $K_3 = 10^5, 10^6, \ldots, 10^{11}, 10^{12}$. Later on, the effects of various parameters of foundation mass, including $\beta = 0, 0.25, 0.5, 0.75$ and 1 are examined. Then, a parametric study will be performed in the subsequent sections in order to investigate the effect of the load velocity, linear stiffness, shear stiffness, and damping of the foundation. The dimensionless foundation coefficients K_1, K_2, and K_3 which are defined as follows is used for investigation (Ferreira *et al.* 2010, Jahromi *et al.* 2013, Liu *et al.* 2017) as

$$K_1 = \frac{k_l B^4}{D}; K_2 = \frac{k_s B^2}{D}; K_3 = \frac{k_{nl} B^6}{D}; D = \frac{Eh^3}{12\left(1-\nu^2\right)} \tag{33}$$

In this section, a model shown in Fig. 5 is used for investigation. The dimensions of the plate are given as 20 m in length (L), 10 m in width (B), and 0.2 m in thickness (h). Young's modulus, Poisson's ratio, the plate mass density is $E = 3.1 \times 10^{10}\,\mathrm{N/m^2}$, $\nu = 0.2$, $\rho = 2500\,\mathrm{kg/m^3}$, respectively. The dynamic foundation properties are assumed by the foundation coefficient $K_1 = 50$, $K_2 = 10$, and the damping coefficient $c_f = 100\ \mathrm{Ns/m^3}$, the ratio of foundation mass density to plate's mass density is given as $\mu = 0.75$. A load $P = 100$ kN moves along the longitudinal centerline of the plates with constant velocity V(m/s). The boundary conditions are simple supports at two short edges (Hughes 1987). In this investigation, the plate is discretized into 20×10 rectangular meshes, in which the aspect ratio of the longest dimension to the shortest dimension of a rectangular element is 1 to increase the accuracy (Logan 2017) and the refinement of the mesh is acceptable to study (Bazeley *et al.* 1965, Irons *et al.* 1972, MacNeal *et al.* 1985,

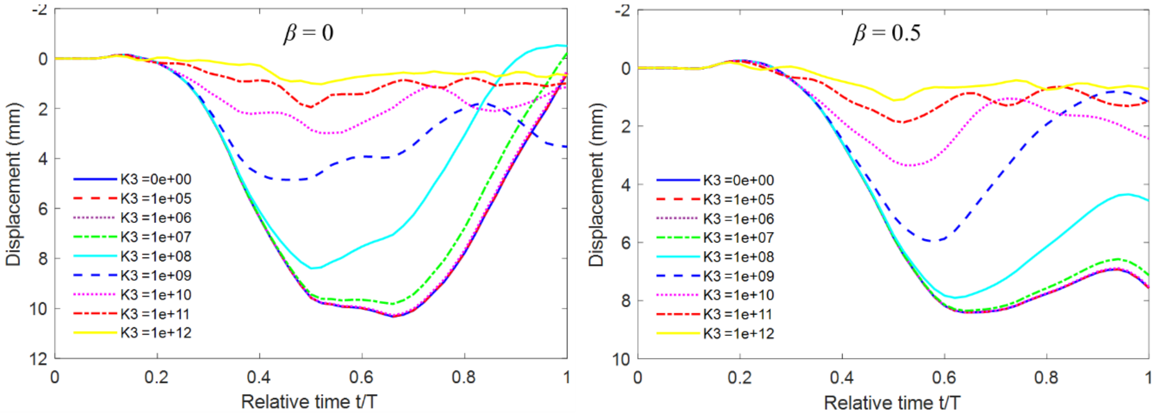

(a) $\beta = 0$ (b) $\beta = 0.5$

Fig. 6 The displacement of the central point of plate for various values of nonlinear stiffness

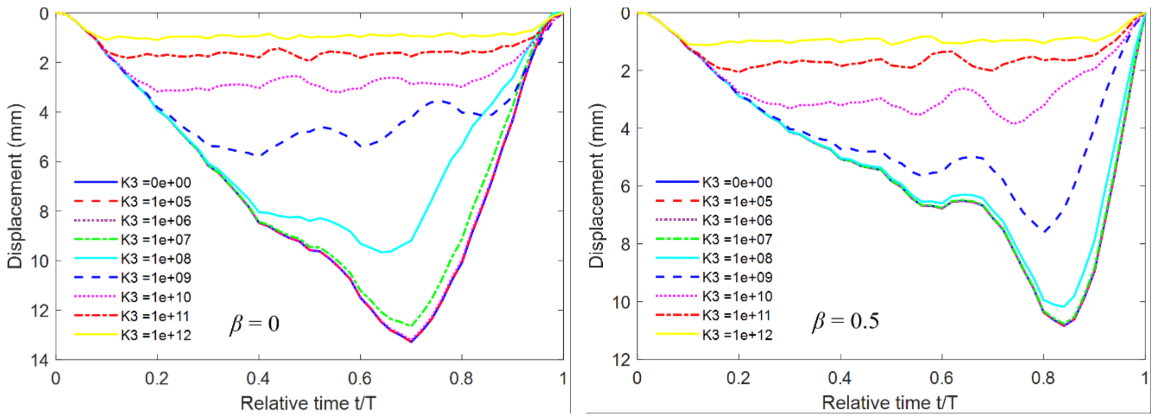

(a) $\beta = 0$ (b) $\beta = 0.5$

Fig. 7 Vertical displacement under moving load for various values of nonlinear stiffness

Taylor *et al.* 1986, Belytschko *et al.* 2000, Cook *et al.* 2002), and 50 time-steps are used in the Newmark-β method.

3.1 The effects of the nonlinear elastic stiffness

The nonlinear stiffness of the foundation are assumed by $K_3 = 10^5, 10^6, \ldots, 10^{11}, 10^{12}$ in two cases of foundation mass: $\beta = 0$ (no considering the foundation mass) and $\beta = 0.5$ (typical case between values of 0 and 1) are chosen correspondingly to the model without and with the effects of the foundation mass. The load's speed $V = 60$ m/s is used in this section. It can be observed from Figs. 6, 7 and 8 that when the nonlinear elastic stiffness of foundation is small ($K_3 \leq 10^7$), the max displacement of plate is not significantly changed because the nonlinear stiffness contributes insignificantly to the global stiffness of the foundation. The max displacement of plate is reduced considerably when the nonlinear stiffness increases and $K_3 \geq 10^8$. Fig. 6 and Fig. 7 show that the displacement curves coincide for various nonlinear stiffness at the early time of

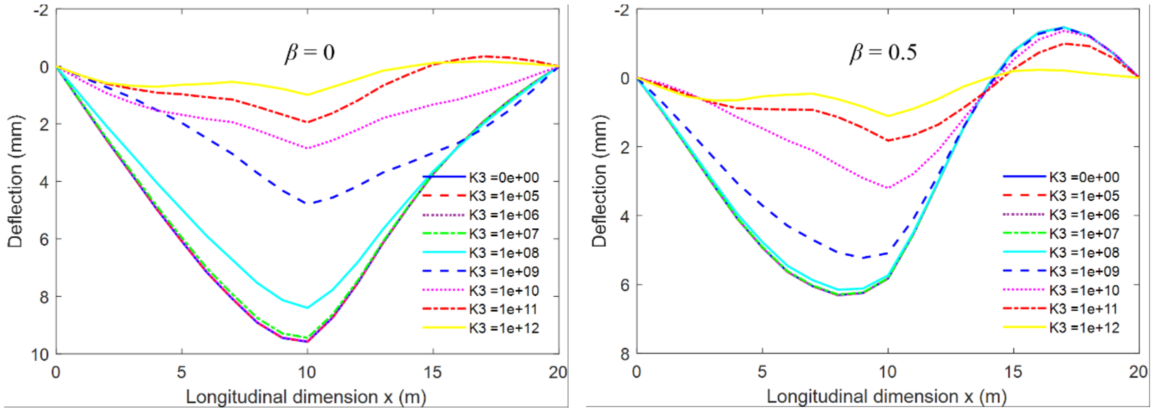

(a) $\beta = 0$ (b) $\beta = 0.5$

Fig. 8 Deflected shapes of longitudinal centerline when a load is at the center for various values of nonlinear stiffness

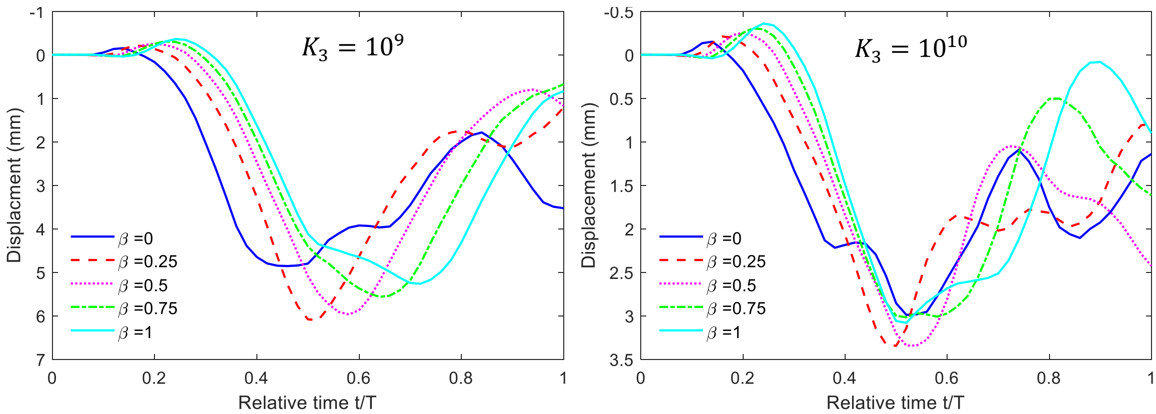

(a) $K_3=10^9$ (b) $K_3=10^{10}$

Fig. 9 The vertical displacement of central point of plate for various foundation mass

load's moving. It can be explained that the displacement of plate is small when the load position is near the first support, thus the effect of the nonlinear stiffness is insignificant. In contrast, when the load position is far from the first support, the vertical displacement of plate increases, while the nonlinear stiffness increases and has a considerable contribution to the total stiffness of the system, thus the displacement curve changes. When the nonlinear stiffness is larger, the increment of displacement stops sooner. The dynamic response of plate changes remarkably when the foundation mass is considered, the displacement of plate at the early time of moving load increases less than the model which excludes the foundation mass. In addition, the peaks of displacement curves under moving load in the model with foundation mass occur later than the mentioned ones of the model without foundation mass.

Fig. 8 shows various shapes of deflection along the centerline of the plate when the moving load arrives at the central point. It is clear that in case the foundation mass is excluded, the max value of deflections occurs at the center of the plate. In contrast, with the inclusion of the

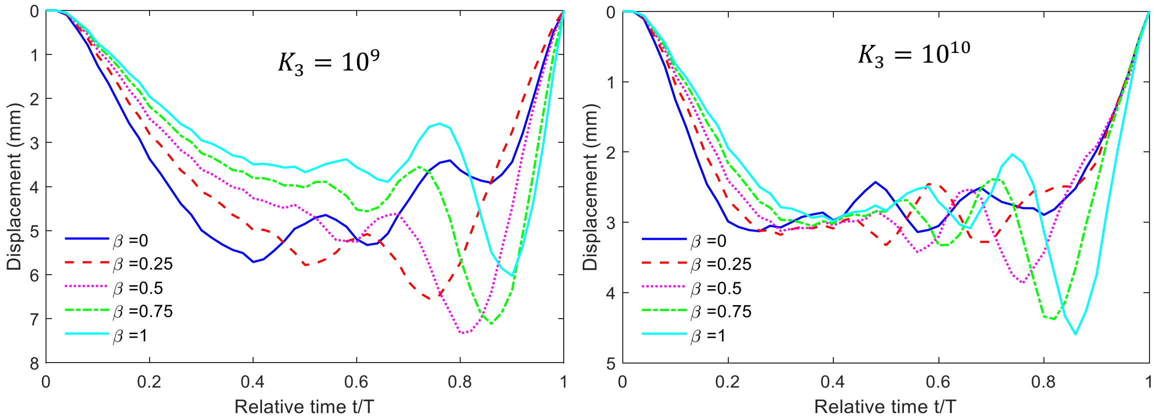

(a) K_3=10^9 (b) K_3=10^{10}

Fig. 10 Vertical displacement under moving load for various foundation mass

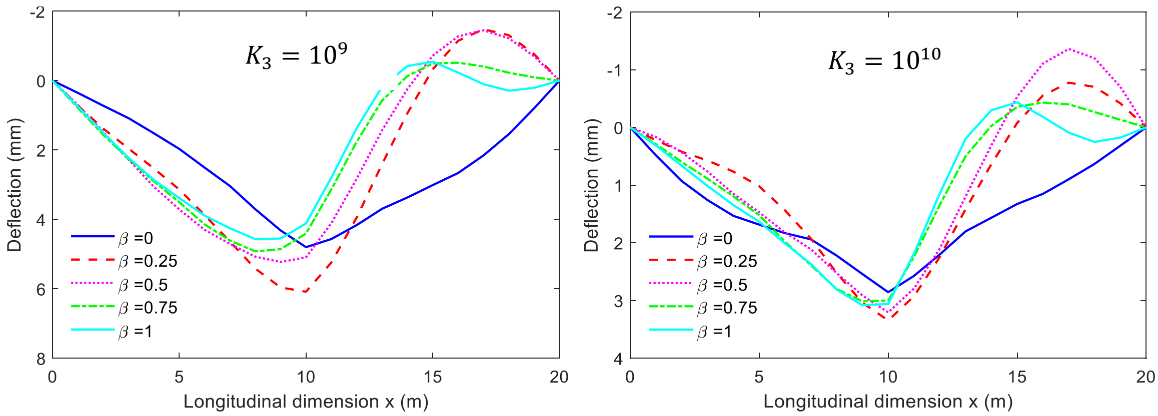

(a) K_3=10^9 (b) K_3=10^{10}

Fig. 11 Deflected shapes of longitudinal centerline when a load is at center for various foundation mass

foundation mass, the max value occurs earlier at the time $\frac{t}{T} < 0.5$ and moves slightly to the center when the nonlinear stiffness of foundation increases.

3.2 The effects of the mass of the foundation

Next, we investigate the effects of five different coefficients of foundation mass $\beta = 0, 0.25, 0.5, 0.75, 1$ in two cases of the foundation's nonlinear stiffness: $K_3 = 10^9$ and $K_3 = 10^{10}$. These two values are chosen for studying since they achieve peak displacements of the nonlinear foundation in the above investigation. The load velocity is kept constant at $V = 60$ m/s in this investigation. It can be seen from Fig. 9 and Fig. 10 that the max vertical displacement of plate increases considerably when the foundation mass is considered in the model. In the first period, the displacement of plate decreases when the foundation mass increases, and the displacement line graph is shifted to the right. It can be explained that the period of vibration of the plate increases

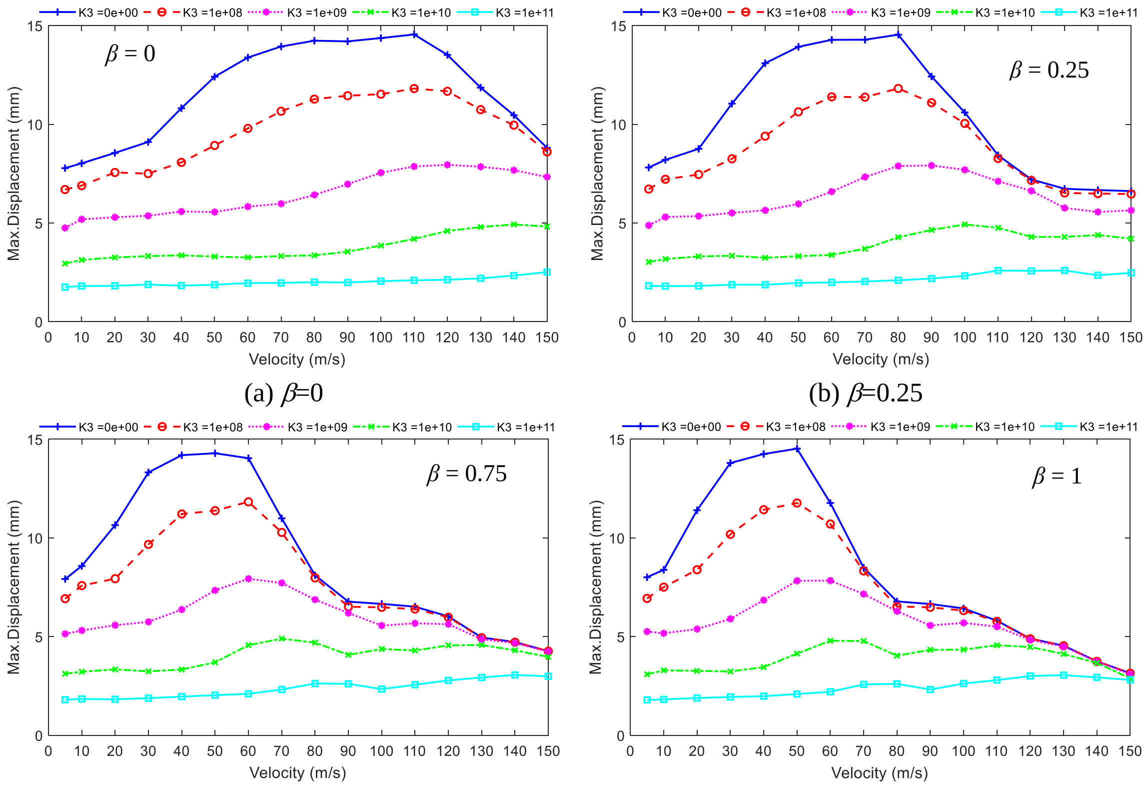

(a) β=0 (b) β=0.25

(c) β=0.75 (d) β=1

Fig. 12 Effects of the varying load velocities and nonlinear stiffness on max displacement

when foundation mass increases. The max displacement does not increase in proportion to the linear increment of the foundation mass, that the effect of the foundation mass on the max displacement also depends on the nonlinear stiffness of foundation.

As shown in Fig. 11, the peak of deflected shape is off to the left side, when the nonlinear stiffness of foundation increases, the peak is closer to the center. When including the foundation mass, the curves on the left are under the line of $\beta = 0$ (the foundation mass is excluded in the model), and the curves on the right are above the line of $\beta = 0$. When the nonlinear stiffness increases, the curves on the left side move closer to the line of $\beta = 0$, while on the right they remain unchanged.

3.3 The effects of the load velocity

First, the various parameters of the load velocity and the nonlinear stiffness are investigated in four different cases of foundation mass: $\beta = 0, 0.25, 0.75$ and 1.

Fig. 12 compares five different nonlinear stiffness of foundation in connection with the max displacement subjects to the various load velocity in the different coefficients of foundation mass. It is apparent that the max displacement of each nonlinear stiffness corresponds to different velocities of moving load. When the nonlinear stiffness is smaller, the lower load velocity will

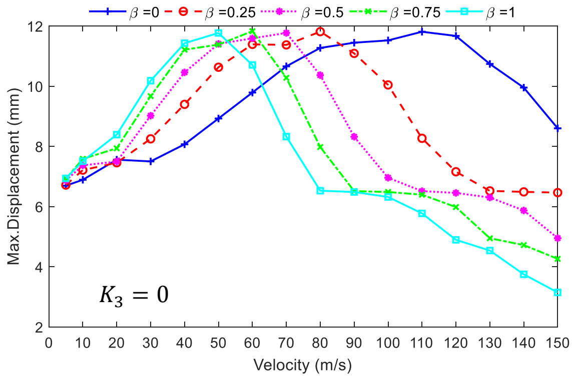

(a) K_3=0

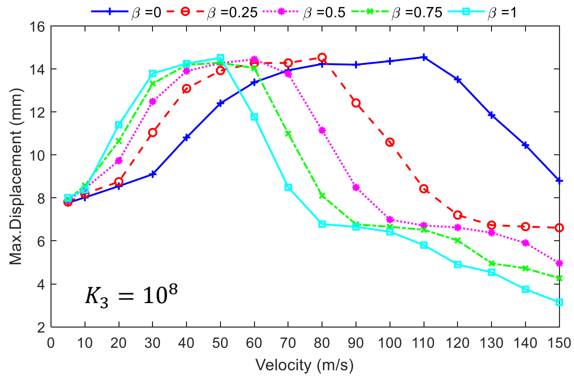

(b) K_3=10^8

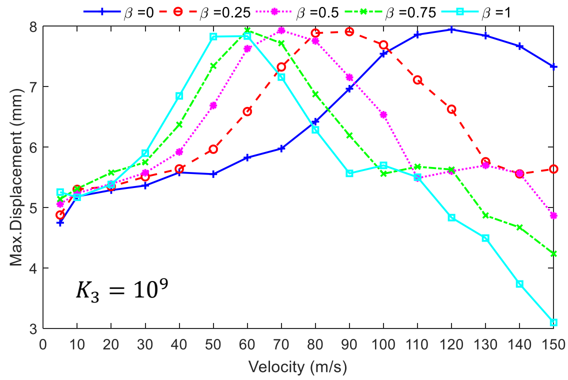

(c) K_3=10^9

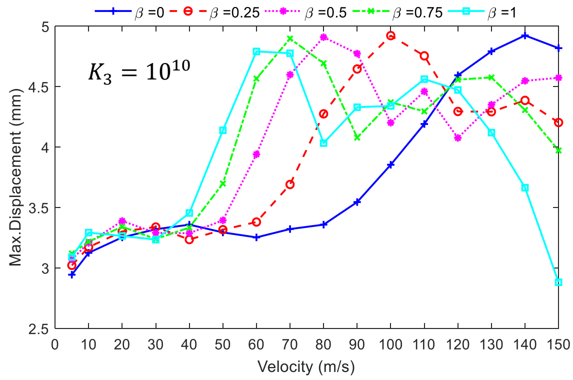

(d) K_3=10^{10}

Fig. 13 Effects of the varying load velocities and foundation mass on max displacement

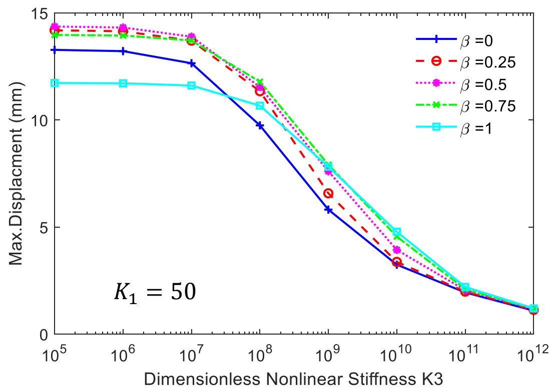

(a) K_1=50

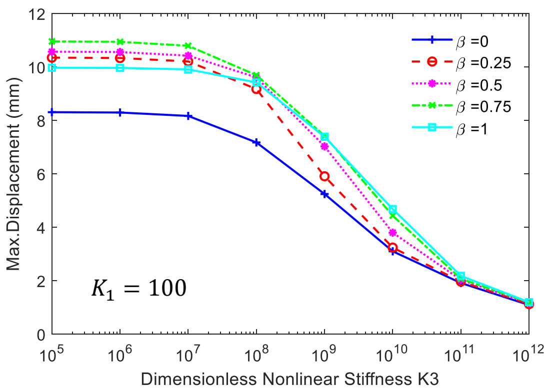

(b) K_1=100

Fig. 14 Effects of linear stiffness on max displacement for various nonlinear stiffness and foundation mass where $K_2 = 10$, $c_f = 100$ Ns/m^3

cause a disadvantage to the structure. It is because when the nonlinear stiffness of the foundation decreases, the frequency of the system will decrease accordingly and resonate with the small value of load velocity. In contrast, when the coefficient of foundation mass increases, the peak of the

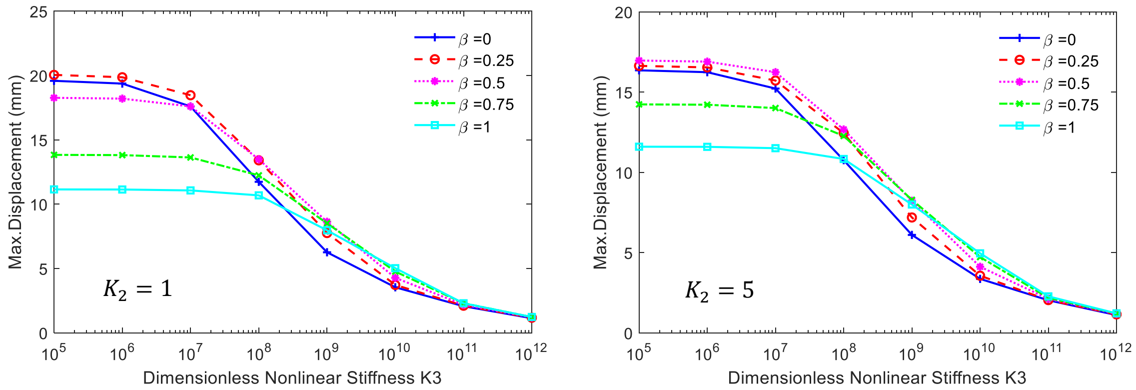

(a) K_2=1 (b) K_2=5

Fig. 15 Effects shear stiffness on max displacement for various nonlinear stiffness and foundation mass where $K_1 = 50$, $c_f = 100$ Ns/m^3

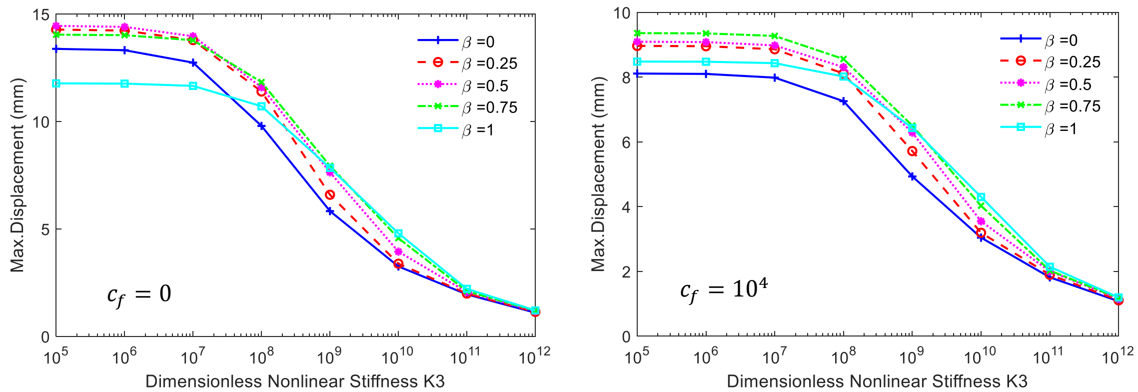

(a) c_f=0 (b) c_f=10^4

Fig. 16 Effects viscous damping of foundation on max displacement for various nonlinear stiffness and foundation mass where $K_1 = 50$, $K_2 = 10$

curve occurs at the smaller load velocity due to the frequency of vibration decreases. The bigger foundation mass, the sharper width of the peak area. The max value is almost equal in all cases, but the corresponding velocity of a moving load is different.

The load velocity and coefficient of foundation mass in four particular cases of the nonlinear stiffness of foundation: $K_3 = 0, 10^8, 10^9$ and 10^{10} are then investigated in this section. Fig. 13 shows a comparison of five particular coefficients of foundation mass in terms of the max displacement over the various load velocity in the different nonlinear stiffness of foundation.

Clearly, the effects of foundation mass are remarkable on the dynamic response of the plate against the load velocity. When the coefficient of foundation mass increases, the peak area of the curve locates at the lower range of load velocity and the width of the peak is noticeably sharp, it is also explained above. In contrast, when the nonlinear stiffness of the foundation increases, the peak of the curve occurs at the higher range of load velocity and the width of the peak area is sharper due to the increasing frequency of vibration. With a similar nonlinear foundation's stiffness, the max value is almost equal, but the corresponding velocity is different.

3.4 The effects of the linear stiffness, shear stiffness, and damping of foundation

We now examine the effects of the mass and nonlinear stiffness in two different cases of the linear stiffness, shear stiffness, and viscous damping, the variations of max vertical displacement of the plate are shown in Figs. 14, 15, and 16, respectively.

In this examination, the load velocity is kept constant at $V = 60$ m/s. It can be seen that the max displacement of plate may increase or decrease the dynamic response of plate when the foundation mass increases, that is depended on the value of nonlinear stiffness, linear stiffness, shear stiffness, and viscous damping. When the nonlinear stiffness, linear stiffness, shear stiffness and viscous damping increase significantly, the foundation mass will amplify the dynamic response of the plates, causing adverse effects.

4. Conclusions

According to the numerical investigation of the Mindlin plate on nonlinear dynamic foundation under moving load for various parameters such as the nonlinear stiffness, coefficient of foundation mass, load velocity, and other parameters, it is possible to conclude as follows

- The foundation mass considerably affects the dynamic response of the plate subjected to moving load, the foundation mass may increase or decrease the max displacement of the plate that depends upon the parameters of the nonlinear stiffness, linear stiffness, shear stiffness, viscous damping of foundation, and the load velocity.
- When the nonlinear stiffness of foundation is small, it shows a minor effect on the dynamic response of the plate, however. When it is sufficient, it will reduce the plate deflection.
- The load velocity affects the dynamic response of the plate. In case the foundation mass is excluded from the model, the influence of the velocity to the max displacement of the plate occurs at higher range than the model considering the foundation mass because the natural frequency of the structure is decreased by the foundation mass. In addition, the displacement of the plate is the same in similar foundation with different parameters of the foundation mass, but the corresponding velocity is different.

References

Abdelghany, S.M., Ewis, K.M., Mahmoud, A.A. and Nassar, M.M. (2015), "Dynamic response of non-uniform beam under moving load and resting on non-linear viscoelastic foundation", *Beni-Suef Univ. J. Basic Appl. Sci.*, **4**, 192-199. https://doi.org/10.1016/j.bjbas.2015.05.007.

Ahmad, F., Jang, T.S., Carrasco, J.A., Rehman, S.U., Ali, Z. and Ali, N. (2018), "An efficient iterative method for computing deflections of Bernoulli-Euler-von Karman beams on a nonlinear elastic foundation", *Appl. Math. Comput.*, **334**, 269-287. https://doi.org/10.1016/j.amc.2018.03.038.

Awodola, T.O. and Adeoye, A.S. (2021), "Vibration of orthotropic rectangular plates under the action of moving distributed masses and resting on a variable elastic Pasternak foundation with clamped end conditions", *Int. J. Adv. Eng. Res. Sci.*, **8**, 26-43.

Bazeley, G.P., Cheung, Y.K., Irons, B.M. and Zienkiewicz, O.C. (1965), "Triangular elements in plate bending-conforming and nonconforming solutions", *Proceedings of the Conference on Matrix Methods in Structural Mechanics*, Dayton, Ohio.

Belytschko, T., Liu, W.K. and Moran, B. (2000), *Nonlinear Finite Elements for Continua and Structures*, Wiley.

Beskou, N.D. and Muho, E.V. (2018), “Dynamic response of a finite beam resting on a Winkler foundation to a load moving on its surface with variable speed”, *Soil Dyn. Earthq. Eng.*, **109**, 222-226. https://doi.org/10.1016/j.soildyn.2018.02.033.

Chien, R.D. and Chen, C.S. (2005), “Nonlinear vibration of laminated plates on a nonlinear elastic foundation”, *Compos. Struct.*, **70**, 90-99. https://doi.org/10.1016/j.compstruct.2004.08.015.

Cook, R.D., Malkus, D.S., Plesha, M.E. and Witt, R.J. (2002), *Concepts and Applications of Finite Element Analysis*, 4th Edition, Wiley, New York.

Daryl, L.M. (2017), *A First Course in the Finite Element Method*, 6th Edition, Cengage Learning.

Ding, H., Chen, L.Q. and Yang, S.P. (2012), “Convergence of Galerkin truncation for dynamic response of finite beams on nonlinear foundations under a moving load’, *J. Sound Vib.*, **331**, 2426-2442. https://doi.org/10.1016/j.jsv.2011.12.036.

Ferreira, A.J.M., Roque, C.M.C., Neves, A.M.A., Jorge, A.M.N. and Soares, C.M.M. (2010), “Analysis of plates on Pasternak foundations by radial basis functions”, *Comput. Mech.*, **46**, 791-803. https://doi.org/10.1007/s00466-010-0518-9.

Froio, D. and Rizzi, E. (2017), “Analytical solution for the elastic bending of beams lying on a linearly variable Winkler support”, *Int. J. Mech. Sci.*, **128**, 680-694. https://doi.org/10.1016/j.ijmecsci.2017.04.021.

Froio, D., Rizzi, E., Simões, F.M.F. and Costa, A.P. (2017), “Critical velocities of a beam on nonlinear elastic foundation under harmonic moving load”, *Procedia Eng.*, **199**, 2585-2590. https://doi.org/10.1016/j.proeng.2017.09.348.

Froio, D., Rizzi, E., Simões, F.M.F. and Costa, A.P. (2018), “Dynamics of a beam on a bilinear elastic foundation under harmonic moving load”, *Acta Mechanica*, **229**(10), 4141-4165. https://doi.org/10.1007/s00707-018-2213-4.

Ghannadiasl, A. and Mofid, M. (2015), “An analytical solution for free vibration of elastically restrained Timoshenko beam on an arbitrary variable Winkler foundation and under axial load”, *Lat. Am. J. Solid. Struct.*, **12**, 2417-2438. https://doi.org/10.1590/1679-78251504.

Huang, M.H. and Thambiratnam, D.P. (2001), “Deflection response of plate on Winkler foundation to moving accelerated loads”, *Eng. Struct.*, **23**, 1134-1141. https://doi.org/10.1016/S0141-0296(01)00004-9.

Huang, M.H. and Thambiratnam, D.P. (2002), “Dynamic response of pates on elastic foundation to moving loads”, *J. Eng. Mech.*, **128**, 1016-1022. https://doi.org/10.1061/(ASCE)0733-9399(2002)128:9(1016).

Hughes, T.J.R. (1987), *The Finite Element Method-Linear Static and Dynamic Finite Element Analysis*, Prentice-Hall, Inc.

Irons, B.M. and Razzaque, A. (1972), “Experience with the patch test for convergence of finite element methods”, *The Mathematical Foundations of Finite Element Method with Applications to Partial Differential Equations*, Academic Press, New York.

Jafari, P. and Kiani, Y. (2022), “A four-variable shear and normal deformable quasi-3D beam model to analyze the free and forced vibrations of FG-GPLRC beams under moving load”, *Acta Mechanica*, **233**(7), 2797-2814. https://doi.org/10.1007/s00707-022-03256-w.

Jafari, P. and Kiani, Y. (2022), “Analysis of arbitrary thick graphene platelet reinforced composite plates subjected to moving load using a shear and normal deformable plate model”, *Mater. Today Commun.*, **31**, 103745. https://doi.org/10.1016/j.mtcomm.2022.103745.

Jahromi, H.N., Aghdam, M.M. and Fallah, A. (2013), “Free vibration analysis of Mindlin plates partially resting on Pasternak foundation”, *Int. J. Mech. Sci.*, **75**, 1-7. https://doi.org/10.1016/j.ijmecsci.2013.06.001.

Jiya, M. and Shaba, A. (2018), “Analysis of a uniform Bernoulli-Euler beam on Winkler foundation subjected to harmonic moving load”, *J. Appl. Sci. Environ. Manage.*, **22**(3), 368. https://doi.org/10.4314/jasem.v22i3.13.

Jorge, P.C., Simões, F.M.F. and Costa, A.P. (2015a), “Dynamics of beams on non-uniform nonlinear foundations subjected”, *Comput. Struct.*, **148**, 26-34. https://doi.org/10.1016/j.compstruc.2014.11.002.

Jorge, P.C., Simões, F.M.F. and Costa, A.P. (2015b), “Finite element dynamic analysis of finite beams on a bilinear foundation under a moving load”, *J. Sound Vib.*, **346**, 328-344.

https://doi.org/10.1016/j.jsv.2014.12.044.
Karahan, M.M.F. and Pakdemirli, M. (2017), "Vibration analysis of a beam on a nonlinear elastic foundation", *Struct. Eng. Mech.*, **62**(2), 171-178. https://doi.org/10.12989/sem.2017.62.2.171.
Kiani, Y. (2017), "Analysis of FG-CNT reinforced composite conical panel subjected to moving load using Ritz method", *Thin Wall. Struct.*, **119**, 47-57. https://doi.org/10.1016/j.tws.2017.05.031.
Kiani, Y. (2017), "Dynamics of FG-CNT reinforced composite cylindrical panel subjected to moving load", *Thin Wall. Struct.*, **111**, 48-57. https://doi.org/10.1016/j.tws.2016.11.011.
Kiani, Y. (2020), "Influence of graphene platelets on the response of composite plates subjected to a moving load", *Mech. Bas. Des. Struct. Mach.*, **50**(4), 1123-1136. https://doi.org/10.1080/15397734.2020.1744006.
Kiani, Y. (2022), "Free and forced vibrations of graphene platelets reinforced composite laminated arches subjected to moving load", *Meccanica*, **57**(5), 1105-1124. https://doi.org/10.1007/s11012-022-01476-x.
Kim, S.M. and McCullough, B.F. (2003), "Dynamic response of plate on vicous Winkler foundation moving loads of varying amplitude", *Eng. Struct.*, **25**, 1179-1188. https://doi.org/10.1016/S0141-0296(03)00066-X.
Li, M.L., Qian, T., Zhong, Y. and Zhong, H. (2013), "Dynamic response of the rectangular plate under moving loads with variable velocity", *J. Eng. Mech.*, **140**(4), 06014001. https://doi.org/10.1061/(ASCE)EM.1943-7889.0000687.
Liu, H., Liu, F., Jing, X., Wang, Z. and Xia, L. (2017), "Three-dimensional vibration analysis of rectangular thick plates on Pasternak foundation with arbitrary boundary conditions", *Shock Vib.*, **2017**, Article ID 3425298. https://doi.org/10.1155/2017/3425298.
MacNeal, R.H. and Harder, R.L. (1985), "A proposed standard set of problems to test finite element accuracy", *Finite Elem. Anal. Des.*, **1**(1), 3-20. https://doi.org/10.1016/0168-874X(85)90003-4.
Mohebpour, S.R. and Ahmadzadeh, P.M.A.A. (2011), "Dynamic analysis of laminated composite plates subjected to a moving oscillator by FEM", *Compos. Struct.*, **93**, 1574-1583. https://doi.org/10.1016/j.compstruct.2011.01.003.
Nguyen, T.P. and Pham, D.T. (2016), "The influence of mass of two-parameter elastic foundation on dynamic response of beams subjected to a moving mass", *KSCE J. Civil Eng.*, **20**(7), 2842-2848. https://doi.org/10.1007/s12205-016-0167-4.
Nguyen, T.P., Pham, D.T. and Hoang, P.H. (2016a), "A dynamic foundation model for the analysis of plates on foundation to a moving oscillator", *Struct. Eng. Mech.*, **59**(6), 1019-1035. https://doi.org/10.12989/sem.2016.59.6.1019.
Nguyen, T.P., Pham, D.T. and Hoang, P.H. (2016b), "A new foundation model of dynamic analysis of beams on nonlinear foundation subjected to a moving mass", *Procedia Eng.*, **142**, 166-173. https://doi.org/10.1016/j.proeng.2016.02.028.
Nguyen, T.P., Pham, D.T. and Hoang, P.H. (2020a), "A nonlinear dynamic foundation model for dynamic response of track-train interaction", *Shock Vib.*, **2020**, Article ID 5347082. https://doi.org/10.1155/2020/5347082.
Nguyen, T.P., Pham, D.T. and Hoang, P.H. (2020b), "Effects of foundation mass on dynamic responses of beams subjected to moving oscillators", *J. Vibroeng.*, **22**(2), 280-297. https://doi.org/10.21595/jve.2019.20729.
Phadke, H.D. and Jaiswal, O.R. (2021), "Dynamic analysis of railway track on variable foundation under harmonic moving load", *J. Rail Rapid Transit.*, **223**(3), 302-316. https://doi.org/10.1177/09544097211020838.
Phadke, H.D. and Jaiswal, O.R. (2021), "Dynamic response of railway track resting on variable foundation using finite element method", *Arab. J. Sci. Eng.*, **45**, 4823-4841. https://doi.org/10.1007/s13369-020-04360-6.
Pham, D.T., Hoang, P.H. and Nguyen, T.P. (2018), "Experiments on influence of foundation mass on dynamic characteristic of structures", *Struct. Eng. Mech.*, **65**(5), 505-512. https://doi.org/10.12989/sem.2018.65.5.505.
Praharaj, R.K. and Datta, N. (2020), "Dynamic response of plates resting on a fractional viscoelastic foundation and subjected to a moving load", *Mech. Bas. Des. Struct. Mach.*, **50**(7), 1-16.

https://doi.org/10.1080/15397734.2020.1776621.

Rodrigues, C., Simões, F.M.F., Costa, A.P., Froio, D. and Rizzi, E. (2018), “Finite element dynamic analysis of beams on nonlinear elastic foundations under a moving oscillator”, *Eur. J. Mech./A Solid.*, **68**, 9-24. https://doi.org/10.1016/j.euromechsol.2017.10.005.

Taylor, R.L., Simo, J.C., Zienkiewicz, O.C. and Chan, A.C.H. (1986), “The patch test-a condition for assessing FEM convergence”, *Int. J. Numer. Meth. Eng.*, **22**(1), 39-62. https://doi.org/10.1002/nme.1620220105.

Teodoru, I.B. and Muşat, V. (2010), “The modified Vlasov foundation model an attractive approach for beams resting on elastic supports”, *Electr. J. Geotech. Eng.*, **15**, 1-13.

Wang, Y. and Kiani, Y. (2022), “Effects of initial compression/tension, foundation damping and pasternak medium on the dynamics of shear and normal deformable GPLRC beams under moving load”, *Mater. Today Commun.*, **33**(1), 104938. https://doi.org/10.1016/j.mtcomm.2022.104938.

Yang, Y., Ding, H. and Chen, L.Q. (2013), “Dynamic response to a moving load of a Timoshenko beam resting on a nonlinear viscoelastic foundation”, *Acta Mechanica Sinica*, **29**(5), 718-727. https://doi.org/10.1007/s10409-013-0069-3.

Yu, H., Yang, Y. and Yuan, Y. (2018), “Analytical solution for a finite Euler–Bernoulli beam with single discontinuity in section under arbitrary dynamic loads”, *Appl. Math. Model.*, **60**, 571-580. https://doi.org/10.1016/j.apm.2018.03.046.

Yu, K., Surianinov, M., Petrash, S. and Yezhov, M. (2021), “Development of an analytical method for calculating beams on a variable elastic Winkler foundation”, *IOP Conf. Ser., Mater. Sci. Eng.*, **1162**(1), 012009. https://doi.org/10.1088/1757-899X/1162/1/012009.

Zhou, S., Song, G., Wang, R., Ren, Z. and Wen, B. (2017), “Nonlinear dynamic analysis for coupled vehicle-bridge vibration system on nonlinear foundation”, *Mech. Syst. Signal Pr.*, **87**, 259-278. https://doi.org/10.1016/j.ymssp.2016.10.025.

CC